DECEMBER 1977 LRP 123/77

# MEASUREMENTS OF DISPERSION RELATION IN ION BEAM-PLASMA SYSTEM

Y. Kawai, Ch. Hollenstein, M. Guyot
and P.J. Paris

Centre de Recherches en Physique des Plasmas

ECOLE POLYTECHNIQUE FEDERALE DE LAUSANNE

# MEASUREMENTS OF DISPERSION RELATION IN ION BEAM-PLASMA SYSTEM

Y. Kawai, Ch. Hollenstein, M.Guyot, and P. Paris

Centre de Recherches en Physique des Plasmas,
Ecole Polytechnique Fédérale de Lausanne,
Lausanne CH-1007, Switzerland

## ABSTRACT

Measurements of the dispersion relation in an ion beam-plasma system are performed. It is found that in the region close to the wave exciter three normal modes, ion acoustic wave, slow and fast ion-beam modes, and in the far region only a wave beat between the slow and fast ion-beam modes exist. An agreement between the experimental results and the theoretical prediction is found.

A number of experiments[1-4] on ion beam-plasma interaction have been made in connection with plasma heating. When an ion beam is injected into an unmagnetized plasma, with a velocity larger than a critical velocity ( $\sim 2\ C_s$) below which the system becomes unstable, three normal modes (ion acoustic wave, slow and fast ion-beam modes) are expected from linear theory. The existence of these three modes has been reported[5] using a DP-machine[6] ($T_e >> T_i$). On the other hand, in the Q-machine experiment[7] where $T_e = T_i$, the beat wave pattern which is produced by interference between the slow and fast ion-beam modes, has been observed. Here, we report that under the condition of $T_e >> T_i$, three normal modes are excited in the region close to the exciter, only the beat wave, which results from the interference between the slow and fast ion-beam modes, is observed in the region far from the exciter. These experimental results are in agreement with the theoretical dispersion relation including the damping rate which has not been discussed so far.

In our experiment, the ion beam-plasma system was synthesized using a DP-device at pressures $< 5 \times 10^{-4}$ Torr (argon gas), $n_e = 10^8 - 10^9$ cm$^{-3}$ and $T_e \lesssim 1$ eV. A positive potential $\Phi$ applied to the driver chamber causes ion flow into the target plasma, producing double-humped ion energy distribution as shown in Fig. 1 (a). The energy of the ion beam was found to vary in proportion to $\phi$ . The density of the target plasma has been kept about one order smaller than that of the driver plasma.

The beam density $n_b$ has been controlled by changing emission currents of the driver plasma source. Movable ion energy analyzer (resolution $\lesssim$ 0.15 eV) and Langmuir probes measure the plasma parameters. To excite the waves, a sinusoidal potential at a frequency $\omega$ is applied to the driver. The amplitude is kept less than 50 mV peak to peak ($\Delta\Phi/T_e \ll 1$), so that we can neglect nonlinear effects[8] as well as ballistic[9] effects[9]. The resulting coherent waves in the target are measured using a Lock-in technique.

We show typical raw data of wave patterns for different $\Phi$ in Fig. 1 (b). The wave frequency is 300 kHz. This figure indicates that for a small beam velocity the wave slowly damps and as the beam velocity is increased, an interference pattern is observed. As shown in Fig. 2 (a), looking carefully at such an interference pattern, it turns out that in the region close to the driver source there are three modes, one of them suffers from a strong damping and in the far region, as a result, the remaining two modes make a beat wave pattern, which seems to be amplitude oscillation[6]. The pitch L of the beat wave decreases with increasing the frequency. However, for $v_b = 1.75\ C_s$, the wave does not show the beat wave pattern as seen in Fig. 2 (b).

Since the observed beat wave is considered to consist of two waves, the dispersion relation of the two waves can be calculated from the pitch L and wavelength $\lambda$ of the beat wave. The damping rate of the two waves was

also estimated from the rate of decrease in maximum envelop amplitude of the beat wave with distance. This method is useful when the waves have almost the same damping rate. The results are shown in Fig. 3. Obviously there are three propagating waves which are almost on the straight lines so that these three waves are considered to be the ion acoustic wave and the slow and fast ion-beam modes.

In order to understand the experimental results, the dispersion relation in an ion beam-plasma system was numerically calculated. When the distribution function of the ion beam is assumed to be a drift-Maxwellian, the dispersion relation can be written[4]

$$\varepsilon(k,\omega)=1-\frac{k^2\lambda_{De}^2}{2}\left\{Z'(x_e)+(1-\alpha)\theta Z'(x_i)+\alpha\theta_b Z'(x_b)\right\}=0 \qquad (1)$$

where $x_j=(\omega/k-v_j)\,/\,(2T_j/m_j)^{\frac{1}{2}}$, j=e, i, b, $\theta=T_e/T_i$, $\theta_b=T_e/T_b$, $\alpha=n_b/n_e$, $m_b=m_i$, and Z' is a derivative of the dispersion function. The numerical results for different beam velocities are shown as solid lines in Fig. 3, where $\theta=10$ and $\theta_b=25$ are taken. In calculating the dispersion relation, the beam velocity $v_b$ was determined from the measured energy distribution, and $\theta$, $\theta_b$ and $\alpha$ were chosen so as to fit the experimental results. The theoretical curves in Fig. 3 (a) correspond to the ion acoustic wave (A) and the slow (S) and fast (F) ion-beam modes, respectively, indicating an agreement with the experimental results. For $v_b=1.8\ C_s$, the excited wave is in agreement with the fast ion-beam mode (F), as seen in Fig. 3 (b).

The theoretical results of the wave damping which is essentially Landau damping will provide important information in understanding wave behaviour like Fig. 2. We show the theoretical values on the right-hand side in Fig. 3. For $v_b = 3.3\ C_s$, both beam modes can propagate with almost the same walength and with a small damping rate while the ion acoustic wave suffers from the strong Landau damping. It was also found from the numerical calculation that when the beam velocity is decreased, the slow ion-beam mode tends to merge into the ion acoustic wave making it unstable. Therefore, the fast ion-beam mode and the unstable ion acoustic wave are expected to be excited. However, in the present experiment, the ion acoustic wave was not observed.

In order to know whether or not the waves can be measured, it will be necessary to take into account an excitation coefficient[10] of the waves together with the dispersion relation. Here, we discuss the excitation coefficient of the excited waves for the large beam velocity, which corresponds to the stable case. Since the excitation coefficient[10] is considered to be nearly proportional to $(\partial\varepsilon/\partial k)^{-1}$, it is easilly shown that the excitation coefficient of the ion acoustic wave is larger than that of the beam modes. Thus, in spite of the stronger damping as shown in Fig. 3 (a), the ion acoustic wave can be observed in the close region because of the large excitation coefficient. In addition to the ion acoustic wave, the slow and fast ion-beam modes are excited so that in the close region three modes propagate and in the far region the slow and fast ion-beam modes propagate, making the beat pattern.

For $v_b = 1.8\ C_s$, theoretically we could have the instability as seen in Fig. 3 (b). However, such an instability was not observed. The reason may be due to the small growth rate and collisional damping which is not included in the calculation. In our experiment, the measurements of the beam energy distribution showed that the decrease in $\Phi$ leads to a decrease in the beam density and hence a decrease of the growth rate.

Important considerations arise from this work. All three normal modes observed here suffer from Landau damping so that the measurements of the wave damping allow us to estimate $\theta$, $\theta_b$ and $\alpha$, and hence $T_i$, $T_b$ and $n_b$, as we have done in Fig. 3. In the case of a small beam velocity as in our experiment, it would be hard to measure the temperature and density of the ion beam by means of the energy analyzer. Therefore, the method used here would be both useful and simple.

We observed the wave beat pattern, which seems to be a nonlinear effect such as the amplitude oscillation. Since the difference of the wavelength between the slow and fast ion beam modes depends on the beam density, the beat wave will be observed especially for a low density beam, which would be easilly realized by an inhomogeneity of the density and potential in the plasma. Therefore, in the experiment the nonlinear effect which one expects to see, should be distinguished from the beat wave.

In summary, when the waves are excited in the ion beam-plasma system, three normal modes, ion acoustic wave, slow and fast ion-beam modes

propagate in the region close to the exciter. In the exciter. In the far region only the beat wave which results from the interference between the slow and fast ion-beam modes. These results can be explained by taking into account the wavelengths and damping rates of the waves and the excitation coefficient.

We would like to thank Professor E.S. Weibel for his encouragement.

This work was supported by the Swiss National Science Foundation.

REFERENCES

1) D.R. Baker, Phys.Rev.Lett. 28, 1189 (1972).

2) R.J. Taylor and F.V. Coronoti, Phys.Rev.Lett. 29, 34 (1972).

3) Y. Kiwamoto, J.Phys.Soc.Jpn. 37, 466 (1974).

4) H.W. Hendel, M. Yamada, S.W. Seiler and H. Ikezi, Phys.Rev.Lett. 36, 319 (1976) ; S.W. Seiler, M. Yamada and H. Ikezi, Phys.Rev.Lett. 37, 700 (1976).

5) D. Grésillon and F. Doveil, Phys.Rev.Lett. 34, 77 (1975).

6) R.J. Taylor, K.R. Mackenzie and H. Ikezi, Rev.Sci.Instrum. 43, 1675 (1972).

7) N. Sato, H. Sugai and R. Hatakeyama, Phys.Rev.Lett. 34, 931 (1975).

8) For example, R.Z. Sagdeev and A.A. Galeev, Nonlinear Plasma Theory, edited by T.M. O'Neil and D.L. Book (Benjamin, New-York, 1969) Chap.II.

9) J.L. Hirshfield and J.H. Jacob, Phys.Fluids 11, 411 (1968).

10) R.W. Gould, Phys.Rev. 136A, 991 (1964).

FIGURE CAPTIONS

Fig. 1 (a) An example of the ion beam energy distribution, where $\Phi$ = 3.5 V.

(b) Typical wave patterns for different potentials $\Phi$, where $\omega/2\pi$ = 300 kHz.

Fig. 2 Wave patterns for (a) $v_b = 3.3\ C_s$ and (b) $v_b = 1.8\ C_s$, where $C_s = 1.4 \times 10^5$ cm/sec.

Fig. 3 Normalized dispersion relation for (a) $v_b = 3.3\ C_s$ and (b) $v_b = 1.8\ C_s$. The solid lines show the theoretical values with $\theta = 10$ and $\theta_b = 25$ for (a) $v_b = 3.3\ C_s$ and $\alpha = 0.3$, and (b) $v_b = 1.8\ C_s$ and $\alpha = 0.05$.

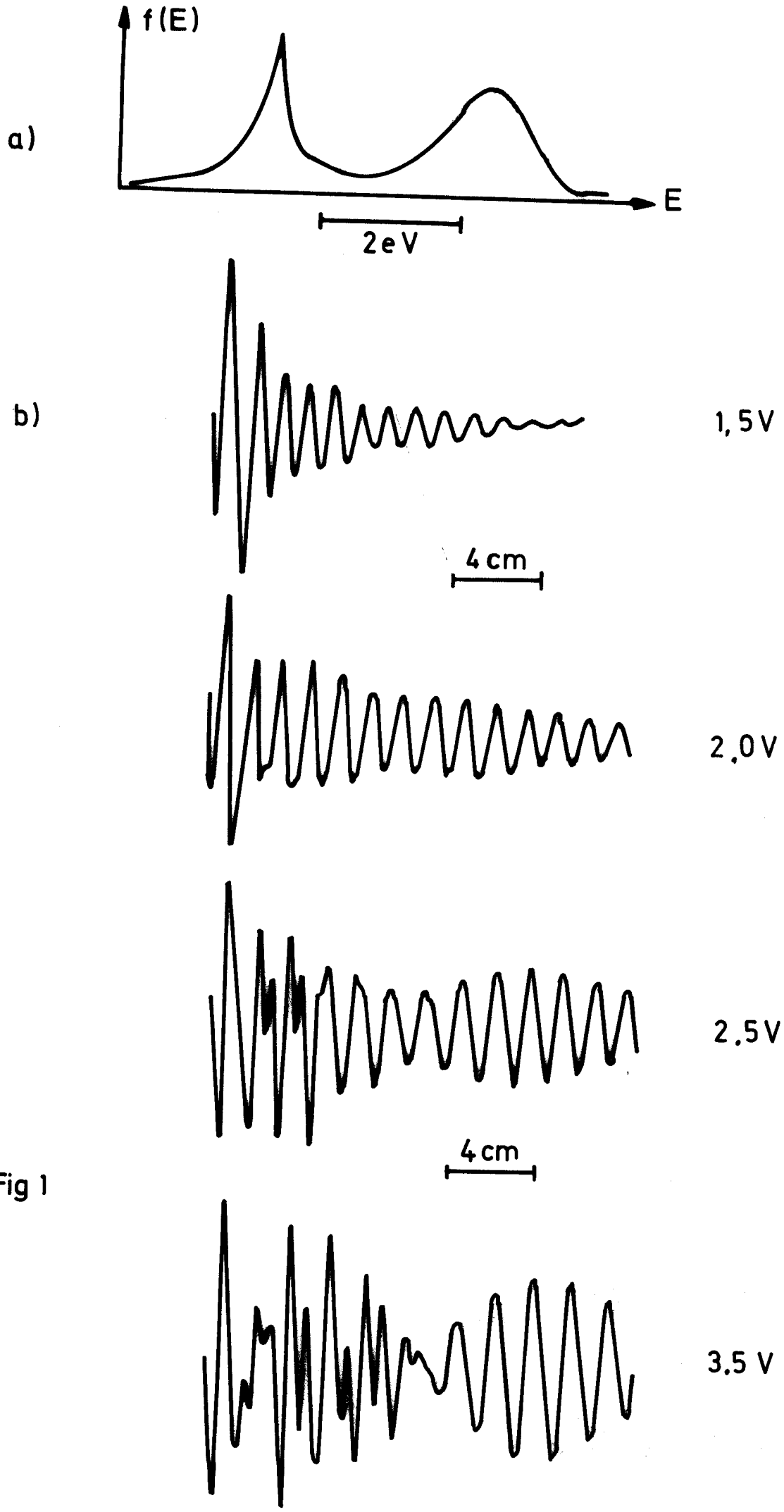


Fig 1

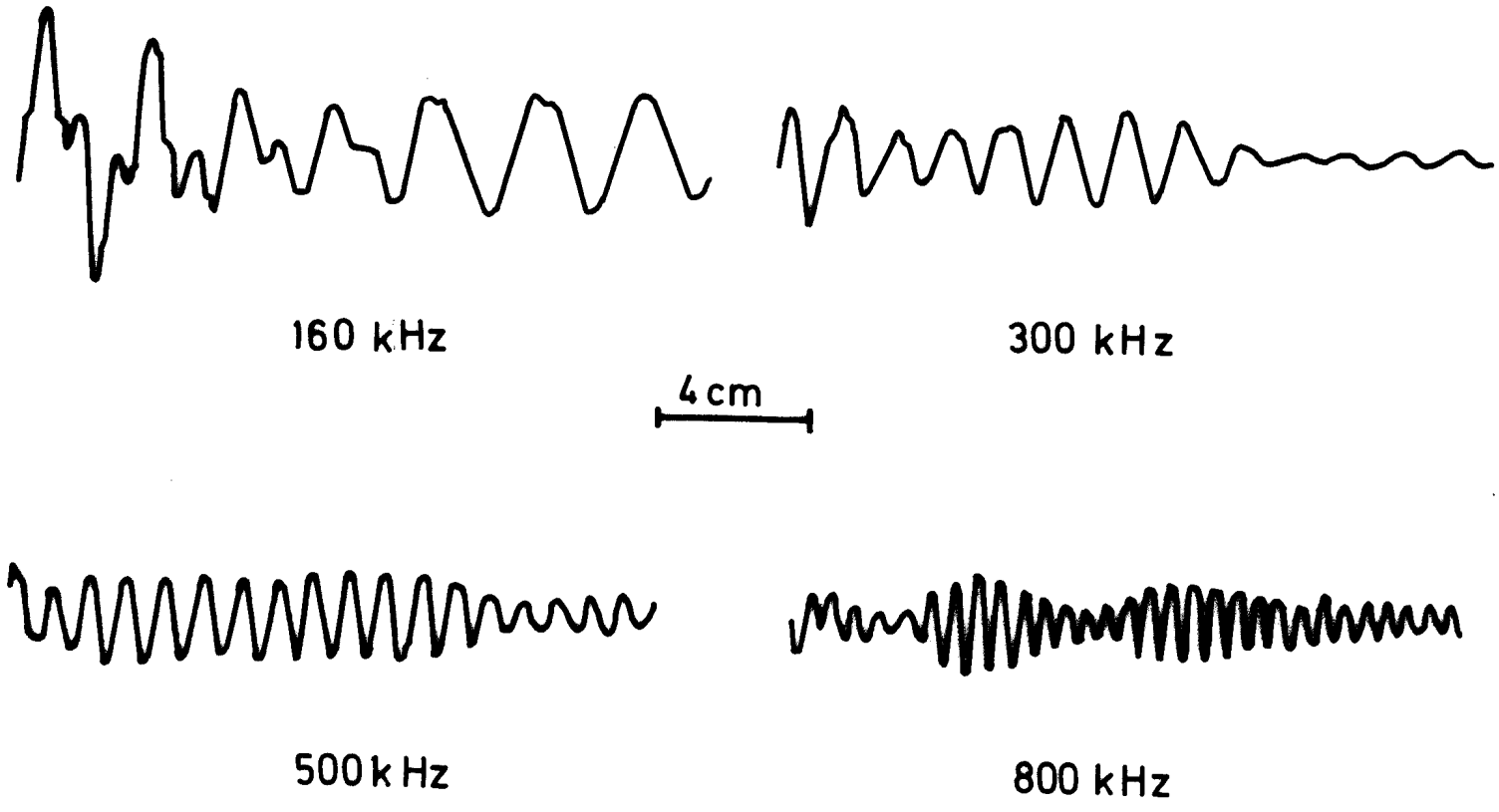
160 kHz
300 kHz
4 cm
500 kHz
800 kHz
a)

Fig. 2

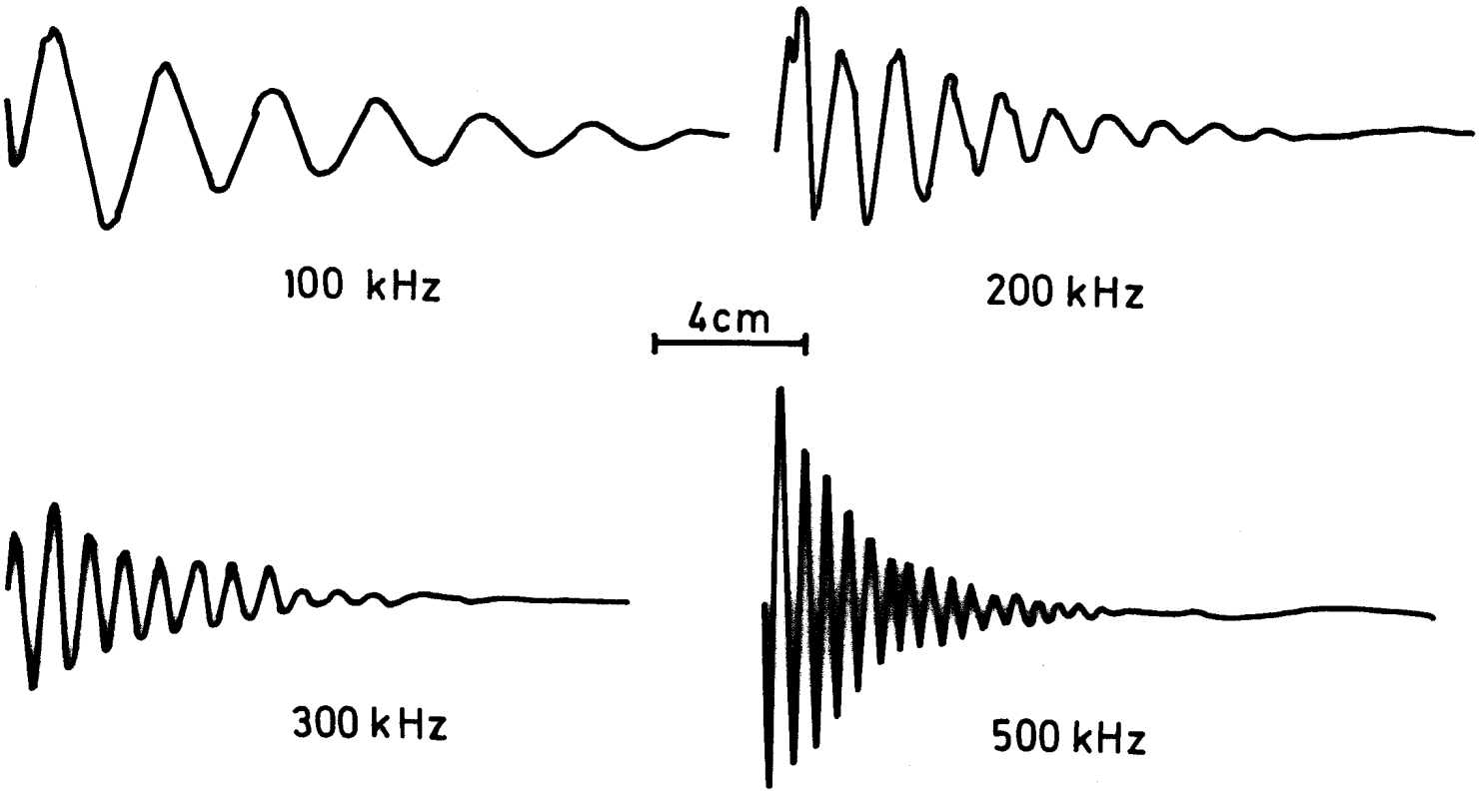
100 kHz
200 kHz
4cm
300 kHz
500 kHz
b)

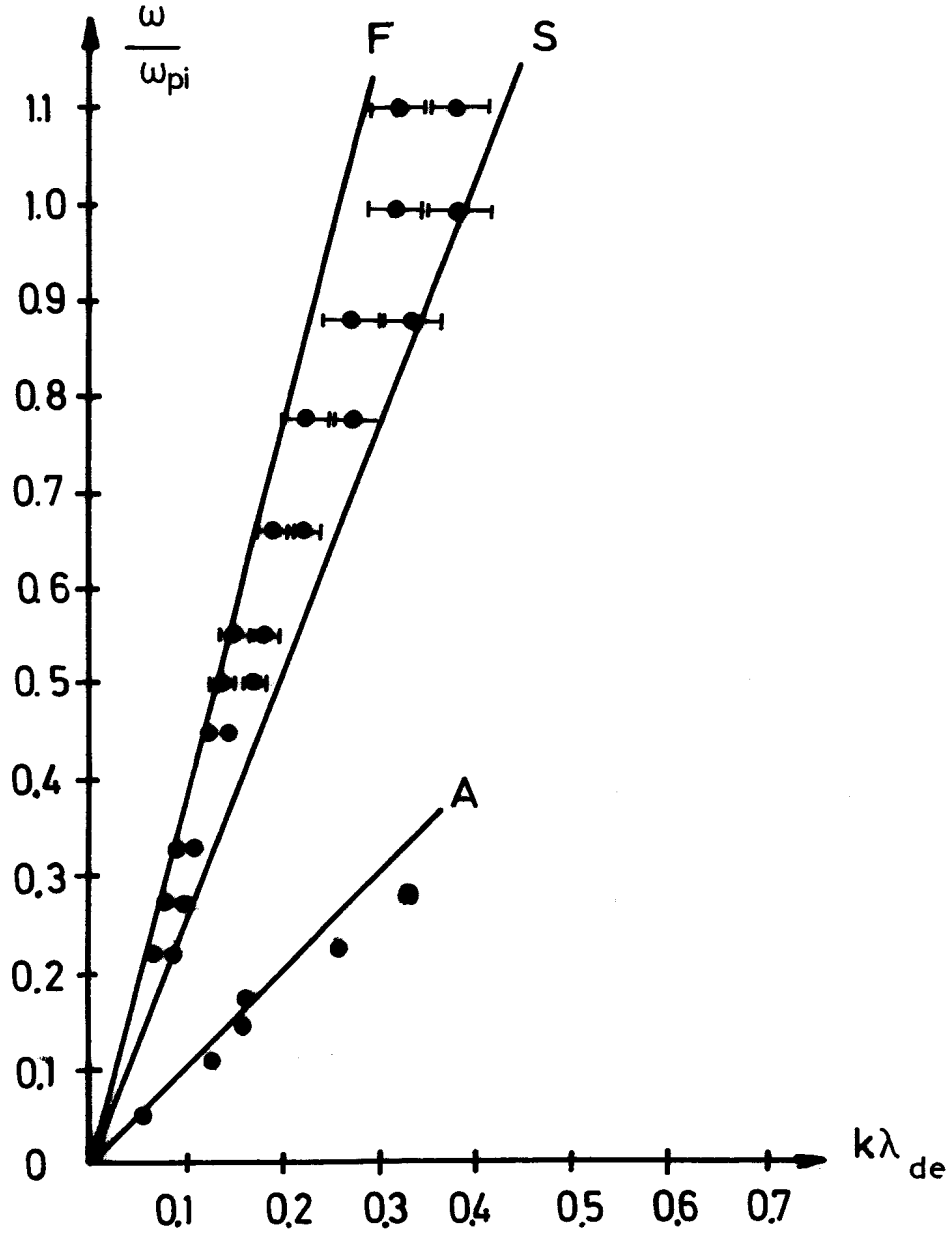
ω/ωpi
F
S
A
1.1
1.0
0.9
0.8
0.7
0.6
0.5
0.4
0.3
0.2
0.1
0
0.1
0.2
0.3
0.4
0.5
0.6
0.7
kλde

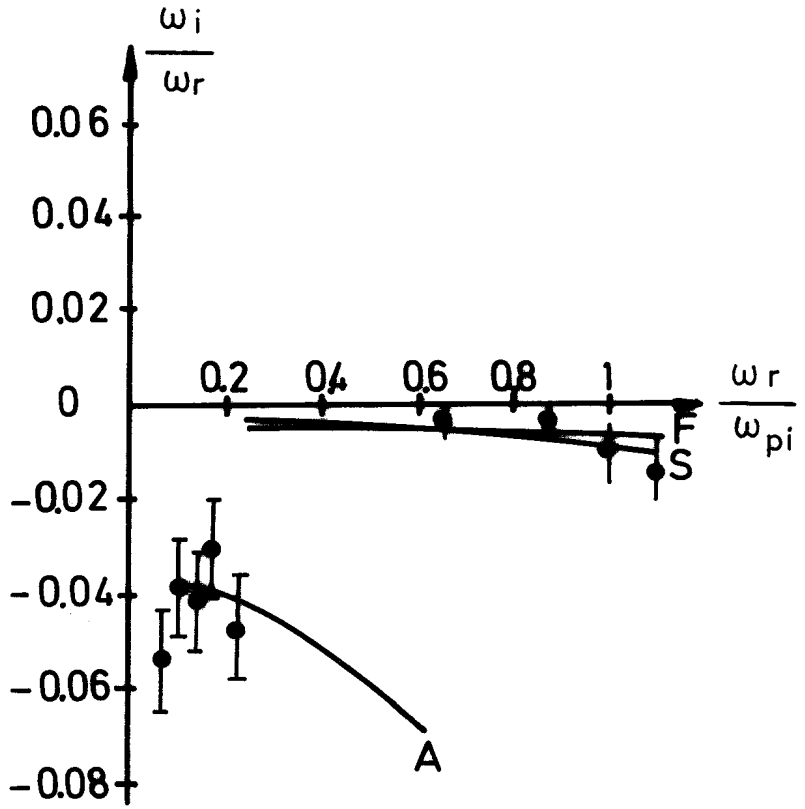
ωi/ωr
0.06
0.04
0.02
0
-0.02
-0.04
-0.06
-0.08
0.2
0.4
0.6
0.8
1
ωr/ωpi
F
S
A

Fig. 3a

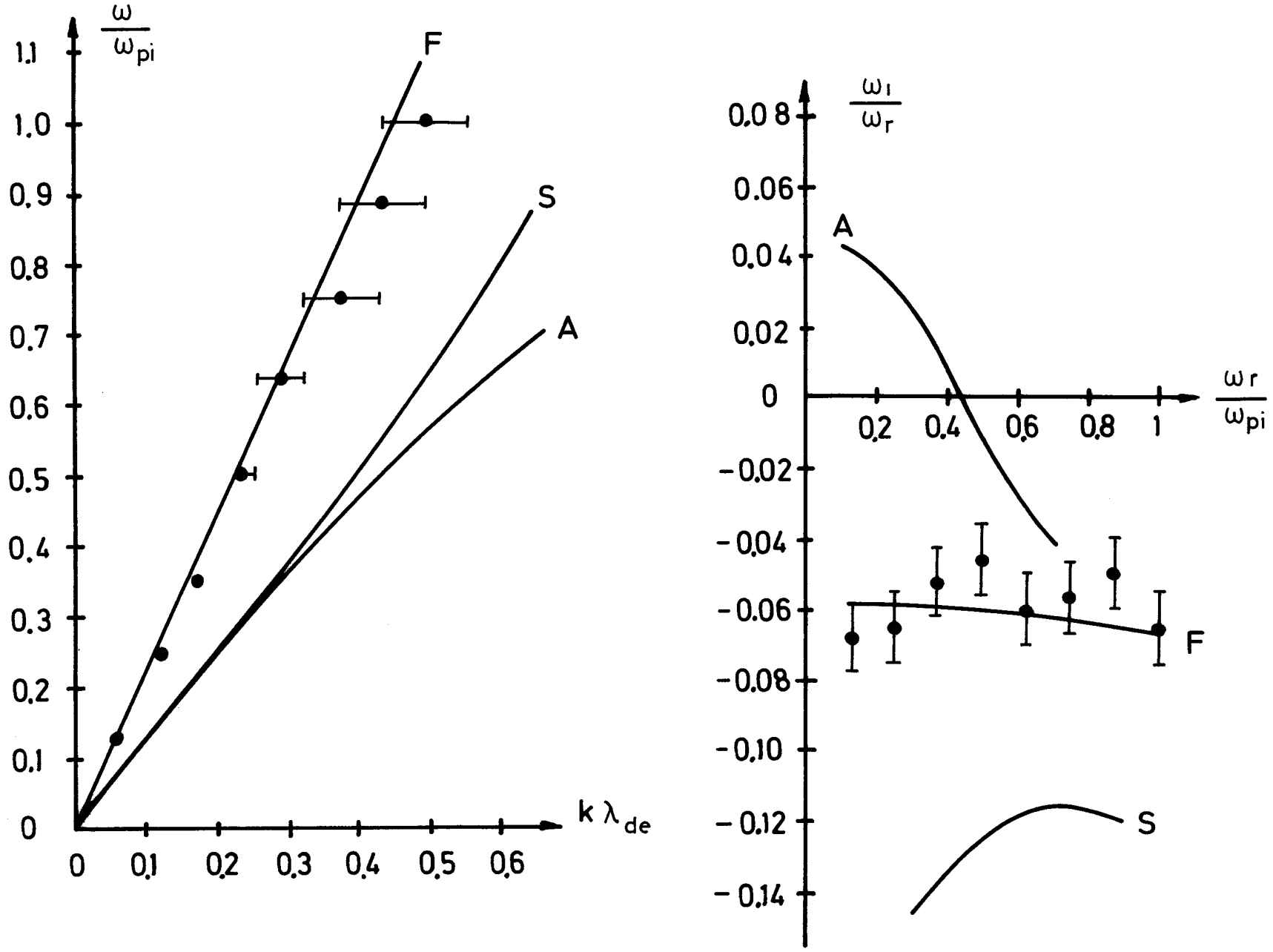
ω/ωpi
1.1
1.0
0.9
0.8
0.7
0.6
0.5
0.4
0.3
0.2
0.1
0
F
S
A
kλde
0
0.1
0.2
0.3
0.4
0.5
0.6
ωi/ωr
0.08
0.06
0.04
0.02
0
-0.02
-0.04
-0.06
-0.08
-0.10
-0.12
-0.14
A
F
S
ωr/ωpi
0.2
0.4
0.6
0.8
1

Fig.3b